Journal of the Brazilian Society of Mechanical Sciences and Engineering (2025) 47:580
https://doi.org/10.1007/s40430-025-05840-2

TECHNICAL PAPER

Enhancing stirring performance through chaotic position control in a magnetic stirrer

Mert Süleyman Demirsoy[1] · Muhammed Salih Sarıkaya[1] · Sedat Kurnaz[2] · Yusuf Hamida El Naser[1] · Mehmet Ali Hazar[3] · Selçuk Coşkun[3] · Mustafa Çağrı Kutlu[1,4] · Gizem Hazar[3]

Received: 26 February 2025 / Accepted: 16 July 2025 / Published online: 2 September 2025

Abstract

This study aims to develop an innovative chaotic magnetic stirrer system to enhance mixture homogeneity and dissolution efficiency. Unlike conventional magnetic stirrers, the proposed system continuously alters the position of the magnetic stir bar based on the Halvorsen, Lorenz, and Sprott-A chaotic equations. This approach prevents the mixture from being confined to a specific region and ensures broader dispersion throughout the solution, thereby achieving a faster homogeneous mixture. The developed chaotic magnetic stirrer was evaluated in the experimental studies compared to a conventional magnetic stirrer. Dissolution efficiency, conductivity, and pH variations were measured, and it was observed that the system operating with the Halvorsen chaotic model achieved the highest dissolution efficiency. In short-term experiments, the Halvorsen model demonstrated an 11.99% improvement in conductivity compared to the conventional method, while the Sprott-A model exhibited a 4.21% enhancement. Specifically in long-term mixing assessments, all chaotic models reached solution saturation significantly earlier than the conventional stirring method. The Halvorsen model achieved saturation at the 150th minute, followed by the Sprott-A model at the 160th minute and the Lorenz model at the 175th minute, whereas the conventional method only reached saturation at approximately the 215th minute. This substantial reduction in time to saturation across all chaotic configurations highlights the effectiveness of chaotic stirring in enhancing mass transfer rates and accelerating solution homogenization. Similarly, pH measurements indicated that chaotic mixing methods, particularly the Halvorsen model, accelerated the dissolution process and facilitated faster attainment of chemical equilibrium. The findings reveal that chaotic magnetic stirrer systems provide more effective mixing and optimize the dissolution process than conventional methods. This study integrates chaos theory, a mathematical phenomenon, into engineering and mixing technologies.

Keywords Magnetic stirrer · Chaos · Position control · Mixture homogeneity · Cartesian platform

1 Introduction

Magnetic stirrers are widely utilized in both laboratory and industrial applications. Fundamentally, they ensure the homogeneous mixing of solutions, thereby facilitating chemical reactions in a uniform and efficient manner. Unlike mechanical stirrers, magnetic stirrers operate without the need for a mechanical agitator, instead they rely on a rapidly rotating magnetic stirring element to effectively mix the materials within a solution. This method significantly reduces the risk of contamination, making it particularly advantageous for experiments involving reactive chemicals and ensuring a safer working environment [1–5].

Literature studies examining various aspects of magnetic stirrers and their impact on mixing efficiency provide valuable insights into enhancing the performance of this technology. Magnetic stirrers have been widely acknowledged for their superior performance over mechanical alternatives in terms of vortex formation, mixing efficiency, and operational simplicity [4, 5]. These systems promote improved flow consistency and reduced maintenance due to their minimal mechanical complexity and adaptability to various container geometries. However, many of these studies do not explore the behavior of magnetic fields under dynamic boundary conditions or the interaction with non-Newtonian fluids, which limits their applicability in complex stirring scenarios [6, 7]. Furthermore, while improved adsorption

Technical Editor: Maira M Silva.

Extended author information available on the last page of the article efficiency and fluid–solid interactions have been documented [8], there remains a gap in understanding the underlying flow behavior and turbulence modulation that drive these effects [8, 9]. Despite their reproducibility and design simplicity, traditional magnetic stirrers are often limited by fixed spatial trajectories and lack of temporal variation, leading to stagnation zones, particularly in non-Newtonian or high-viscosity fluids [10, 11]. Variable-speed stirring has shown promise in mitigating these issues, improving fluid homogeneity and tailoring conditions to different rheological profiles [12]. However, long-term phase behavior, structural integrity, and microstructural evolution remain insufficiently studied [12, 13]. In pharmaceutical and chemical processing, magnetic stirring has demonstrated benefits for enhancing mass transfer and dissolution rates, yet these studies seldom evaluate the role of stirrer positioning, orientation, or field dynamics [14–16].

Dynamic flow control (particularly through chaotic motion) has emerged as a novel strategy to overcome these limitations. Chaotic actuation enables unpredictable, space-filling trajectories that disrupt stable flow lines and improve mixing uniformity. Empirical studies have validated these methods by showing improved hydrate dissociation [17], accelerated mass transfer [18], and enhanced reaction kinetics in both Newtonian and non-Newtonian systems [19]. Variable-speed chaotic strategies also hold promise in applications where constant flow fails to achieve optimal solute dispersion or chemical equilibrium [20, 21]. Chaotic mixing has further proven effective in modulating fluid behavior at micro- and macro-scales. Its role in eliminating dead zones and improving energy distribution has been substantiated in systems ranging from microdroplet reactors to industrial polymer mixers [21–25]. Experiments with double-stirrer setups and robotic platforms have also revealed that chaotic positioning of stirrers greatly enhances turbulence and uniformity within the medium [26, 27]. These insights have been extended to nanocomposites and solid–liquid mixtures, where chaotic dynamics have been linked to enhanced conductivity, structural reinforcement, and fracture resistance [28, 29]. Moreover, computational studies employing chaotic attractors systems illustrate the effectiveness of nonlinear modulation in improving material dispersion and system responsiveness [30, 31]. In solid–liquid processing, chaotic kinematics embedded in robotic arms have been shown to outperform traditional rotary mechanisms in terms of uniform dispersion [32]. Fractal impellers and chaotic porous geometries have similarly demonstrated an ability to generate complex flow regimes that support high reaction rates and low energy requirements [33, 34].

Further validation comes from empirical studies that link chaotic stirring to measurable improvements in solubility and dissolution behavior. Enhanced ionic interactions and disrupted solute clustering mechanisms under chaotic conditions have enabled more efficient molecular dispersion [35, 36]. These outcomes align with macro-scale flow studies that report improved channel utilization and vortex deformation through non-repetitive motion profiles [37]. Researchers have also identified that chaotic advection improves gasoline–water blending and other immiscible systems by generating small-scale instabilities that boost mixing efficiency [38]. In high-viscosity conditions, chaotic geometries have been observed to prevent stagnation by enabling three-dimensional stretching and folding of flow lines [39]. The use of biharmonic equations in extruder design has produced nonlinear trajectories that support more efficient mixing with reduced energy input [40]. Similarly, chaotic mixers operating in polymeric and porous environments have demonstrated significant reductions in processing time while maintaining product quality [41, 42]. These findings are reinforced by comparative studies revealing that chaos-induced structures outperform traditional laminar or turbulent regimes across various performance metrics [43].

Recent investigations have begun evaluating chaotic motion-based systems directly against traditional magnetic stirrers. A notable study utilizing an impinging-jets microreactor (which inherently induces chaotic flow) demonstrated enhanced rheological behavior and sol formation compared to magnetic stirring [44]. While traditional stirrers maintain consistent but spatially limited shear zones, chaotic reactors showed more homogeneous particle dispersion and improved nucleation control [39]. Despite these promising results, such comparative studies remain scarce. Additional analyses involving double-stirrer chaos-induced setups have shown that controlled positioning can manipulate flow fields for optimal chaotic advection, yet these configurations are rarely benchmarked against fixed-position magnetic stirrers [16, 45–47]. Likewise, electromagnetic stirring systems incorporating position, frequency, and current modulation have been shown to improve fluid engagement in complex environments, indicating that position-controlled methods may overcome the rigidity of traditional magnetic setups [45]. Experimental evidence also points to structural limitations in fixed magnetic stirrers, such as the formation of stable vortices that trap solutes near the core further underscoring the importance of dynamic repositioning capabilities [45]. In conclusion, while conventional magnetic stirrers offer simplicity and reliability, the literature increasingly points toward chaotic, position-controlled, and nonlinear stirring systems as next-generation alternatives. These approaches overcome spatial stagnation, enhance mixing uniformity, and support adaptive energy distribution making them especially well-suited for complex, applications where traditional methods fall short [33–45]. Numerous studies have demonstrated that the choice of mixing technique and operating conditions directly impacts solubility, mixture homogeneity, processing duration, and overall system efficiency. Among these, chaotic mixing approaches have shown notable advantages, particularly in enhancing dispersion quality and dissolution rates in both liquid–liquid and solid–liquid systems [21–27].

Despite the practical benefits of conventional magnetic stirrers (such as ease of use, low maintenance, and broad applicability) several limitations persist. These include the formation of localized vortices that hinder complete mixing, particle sizes and the inefficiency of fixed stirrer positioning, which can lead to incomplete dissolution and reduced chemical performance. Such drawbacks underscore the need for advanced stirring mechanisms capable of overcoming spatial and dynamic constraints. To overcome the limitations of conventional magnetic stirring systems, this study proposes an innovative design that integrates chaos theory into stirring dynamics. In the developed system, the spatial position of the magnetic stir bar is dynamically altered using nonlinear chaotic trajectories derived from Halvorsen, Lorenz, and Sprott-A attractors. Unlike the fixed-position magnetic stirrer bar in conventional magnetic stirrers, the chaotic motion continuously repositions the vortex-inducing region across the fluid domain, eliminating stagnant zones and enhancing local turbulence. This approach appears particularly promising for laboratory-scale processes involving low-viscosity solvents or solutes with slow dissolution kinetics. The continuous modulation may strengthen convective transport mechanisms and promote more uniform solute dispersion throughout the medium. Preliminary findings suggest that the proposed system can improve conductivity and pH uniformity, reduce homogenization time, and potentially enhance the overall efficiency, reliability, and reproducibility of physicochemical experiments. Thus, the study contributes both a technological advancement in magnetic stirring systems and a scientific investigation into the role of chaotic dynamics in process optimization.

The paper is structured as follows: Sect. 2 provides a detailed overview of chaos theory, mechanical components, and hardware aspects, followed by a summary of the experimental procedure steps. Section 3 presents and discusses the experimental results. Finally, Sect. 4 summarizes the findings and offers recommendations for future research.

2 Theoretical background and experimental setup

Various studies have been conducted on the chaotic utilization of magnetic stirrer speeds to improve mixture homogeneity through magnetic stirring. Accordingly, this section first provides a general overview of chaos theory, followed by a detailed examination of the design of the developed device and the experimental procedure.

2.1 Chaos theory

Chaos theory constitutes a mathematical framework for describing the intricate, often unpredictable behavior of nonlinear dynamical systems. Contrary to the colloquial use of the term "chaos," which suggests randomness or disorder, chaotic systems are inherently deterministic, governed by underlying mathematical laws, yet capable of producing highly complex and irregular outcomes under specific conditions [48–50]. These systems, while structured, exhibit behavior that is extremely sensitive to initial conditions, leading to exponentially diverging trajectories over time an essential characteristic often referred to as the "butterfly effect", famously demonstrated by Lorenz during his early work on weather prediction models [50]. The scientific exploration of chaotic behavior dates back to Van der Pol and Van der Mark, who, in 1927, observed irregular oscillations in neon bulb circuits, describing the phenomenon as "anarchy" or "noise" [51–53]. These observations later laid the foundation for modern chaos theory, which now plays a pivotal role in explaining irregular behaviors across diverse fields including meteorology, fluid dynamics, economics, and even biological systems such as heart rhythm irregularities [54, 55]. A key concept in the study of chaos is sensitivity to initial conditions, wherein infinitesimal differences in starting states can lead to vastly different system evolutions [50, 56]. This property implies that long-term prediction becomes virtually impossible, even though the system is governed by well-defined rules. Another defining feature of chaotic systems is their deterministic randomness they are not stochastic, but their behavior mimics randomness due to the nonlinear structure of the governing equations [57]. These equations, often composed of nonlinear differential terms, resist closed-form analytical solutions and instead exhibit dynamic evolution in phase space characterized by strange attractors and fractal geometry. A powerful mathematical model to conceptualize chaotic mixing behavior is the Baker's Transform, which emulates the process of dough folding. Through iterative stretching and folding operations, the transform illustrates how nearby points can diverge significantly over time, thereby promoting uniform dispersion and demonstrating the core mechanism of chaos-induced mixing [58]. This principle has significant implications in engineering domains such as microfluidics and industrial material mixing, where achieving homogeneity is critical [22, 59, 60]. The chaotic advection generated by such transformations disrupts laminar flow patterns and eliminates stagnant regions, thereby enhancing transport phenomena.

One of the fundamental tools employed to diagnose chaotic behavior in dynamical systems is the calculation of Lyapunov exponents. These exponents quantitatively characterize the average rate at which nearby trajectories in the system's phase-space diverge or converge over time.

A positive maximum Lyapunov exponent is a definitive indicator of sensitivity to initial conditions (a hallmark of deterministic chaos) implying that even infinitesimally close starting points will evolve into significantly different states as time progresses [55]. This metric thus serves as a rigorous criterion for identifying chaotic dynamics within nonlinear systems. In the existing literature, numerous well-established chaotic systems have been extensively analyzed using Lyapunov exponents to confirm their chaotic nature. Notably, the Halvorsen, Lorenz, and Sprott-A systems are among the most frequently studied due to their rich phase-space structures and diverse nonlinear characteristics. Each of these systems exhibits at least one positive Lyapunov exponent, affirming their sensitivity to initial conditions and validating their classification as chaotic attractors. Their distinct dynamical behaviors (ranging from the symmetric butterfly-shaped trajectories of the Lorenz system to the more densely packed and irregular trajectories of the Halvorsen system) highlight the wide variety of chaotic motion that can arise from relatively simple nonlinear equations.

In the literature, several widely studied chaotic systems, including the Halvorsen, Lorenz, and Sprott-A systems, are utilized in the positional variations of the developed device. The mathematical models of these chaotic systems are provided in Eqs. (1), (2), and (3), respectively.

$$\begin{aligned} \dot{x} &= ax + by + cz - y^2 \\ \dot{y} &= ay + bz + cx - z^2 \\ \dot{z} &= az + bx + cy - x^2 \end{aligned} \tag{1}$$

The coefficients of the Halvorsen mathematical model presented in Eq. (1) are a = − 1.27, b = − 4, c = − 4 and the initial conditions are defined as x(0) = -5, y(0) = 0 and z(0) = 0. The Halvorsen system exhibits a highly dispersive chaotic attractor due to the presence of quadratic nonlinear damping terms (e.g., $-x^2, -y^2, -z^2$). These nonlinear terms introduce asymmetry and result in irregular, widespread trajectories in the phase space. Such behavior is particularly beneficial in stirring applications, as it facilitates broad coverage of the mixing domain and mitigates stagnation near the beaker walls or at the fluid surface.

$$\begin{aligned} \dot{x} &= a(y - x) \\ \dot{y} &= x(b - z) - y \\ \dot{z} &= xy + cz \end{aligned} \tag{2}$$

The coefficients of the Lorenz mathematical model presented in Eq. (2) are a = 10, b = 28, c = − 8/3 with the initial conditions defined as x(0) = 0, y(0) = − 0.1 and z(0) = 9. The Lorenz system is the most well-known chaotic system and was originally developed to model atmospheric convection. It is characterized by a symmetric double-lobed attractor, where trajectories alternate between two regions of attraction. Although it produces complex, bounded motion, its structure often results in the stirrer spending extended time in either lobe before transitioning leading to periods of localized motion and reduced global coverage compared to the Halvorsen model.

$$\begin{aligned} \dot{x} &= y \\ \dot{y} &= -x + y \cdot z \\ \dot{z} &= 1 - y^2 \end{aligned} \tag{3}$$

The initial conditions of the Sprott-A mathematical model presented in Eq. 3 are defined as x(0) = 0,y(0) = 0.5 and z(0) = 0. The Sprott-A system belongs to a family of simple chaotic systems introduced by Sprott with minimalistic nonlinear terms. Despite its simplicity, it generates a robust chaotic attractor and is particularly attractive for real-time implementation due to its low computational complexity. The absence of squared or cubic nonlinearities in the core equations reduces the integration load, making it well-suited for embedded systems or applications requiring fast feedback.

The Halvorsen chaotic model exhibits a higher degree of dynamical complexity compared to the Lorenz and Sprott-A models. This enhanced complexity stems from the inherent structure of the Halvorsen equations, where nonlinear interactions and coupling mechanisms are more intricate than those observed in the comparatively simpler Lorenz system characterized by its classical double-wing attractor or in the lower-dimensional dynamics of the Sprott-A system. Moreover, the complexity of the Halvorsen attractor is further evidenced by the relatively high sensitivity of its global dynamics to simple parameter modifications. This results in a broader and more diverse set of possible trajectories and bifurcation pathways. Such richness in the dynamical behavior of the Halvorsen attractor results in greater complexity compared to the Lorenz and Sprott-A systems, thereby posing more substantial challenges for synchronization, prediction, and control. These findings emphasize the importance of model selection and parameter tuning in the analysis and application of chaotic systems, and they highlight the crucial role of nonlinear coupling structures in shaping the complexity of dynamical behaviors [61].

The phase portraits of the chaotic system equations presented above are shown in Fig. 1 for Halvorsen, Fig. 2 for Lorenz, and Fig. 3 for Sprott-A.

2.2 System design

This section presents a comprehensive analysis of the mechanical design and motion mechanism of the developed magnetic stirrer device. It elaborates on the fundamental working principle of the system, detailing the motion control

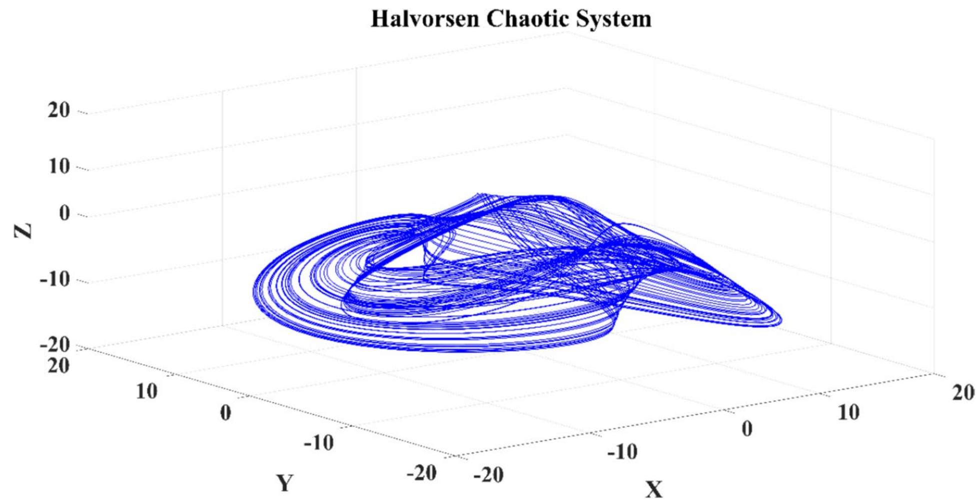

Fig. 1 Phase portraits of the Halvorsen chaotic system

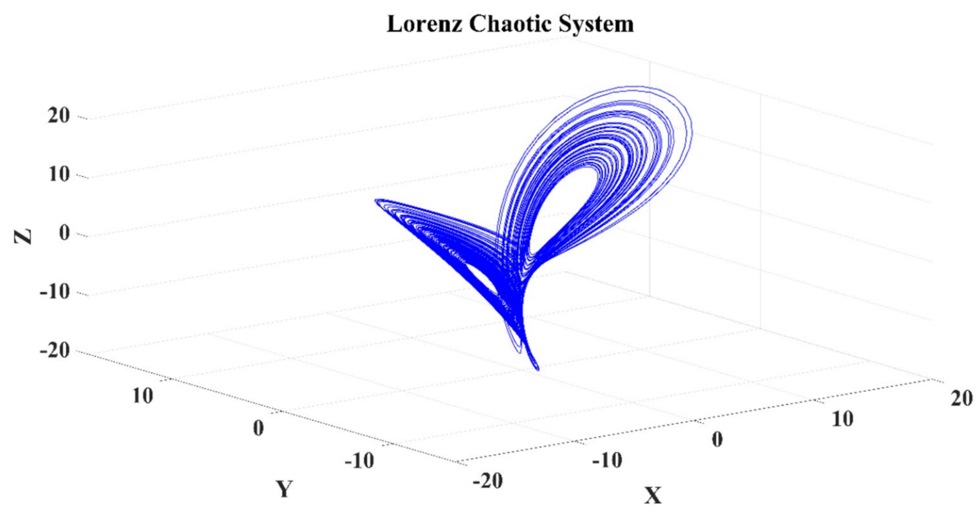

Fig. 2 Phase portraits of the Lorenz chaotic system

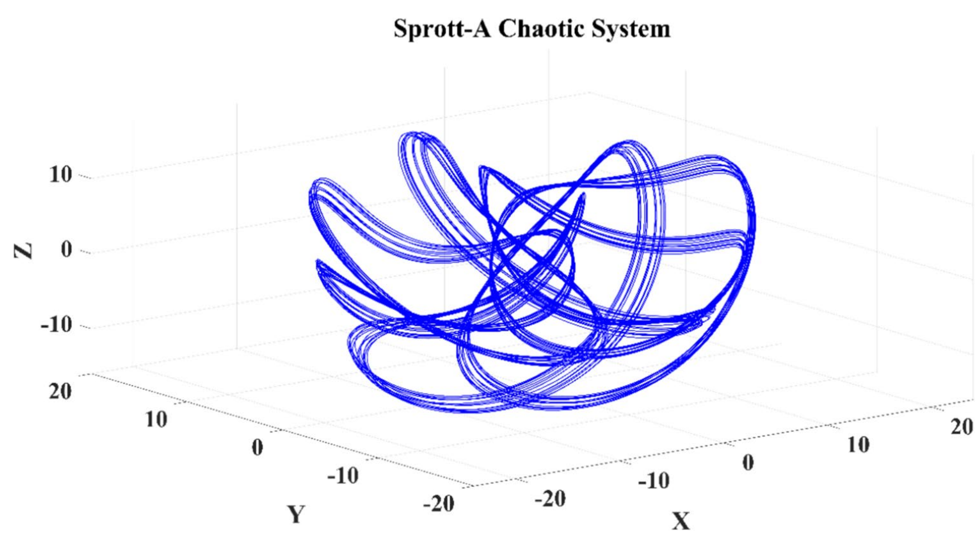

Fig. 3 Phase portraits of the sprott-A chaotic system

mechanisms and the integration of the chaotic motion algorithm to enhance its functionality and efficiency.

The proposed device in this study consists of a gantry platform positioned on linear guide rails, enabling linear motion. A direct current (DC) motor is mounted on the gantry platform, with a magnet attached to its shaft. When the DC motor rotates at a specific angular velocity, the magnet rotates at the same speed, inducing rotation of the magnetic stir bar inside the beaker. This mechanism facilitates effective mixing of the liquid solution. The Cartesian platform design of the mechanism is illustrated in Fig. 4.

The device enables movement along the *X* and *Y* axes of the beaker. The linear motion of the beaker along these two axes is achieved via two stepper motors integrated into the system. Motion transmission is facilitated through a single belt mechanism, ensuring smooth and vibration-free operation via pulleys and roller bearings incorporated within the system. The operational workspace of the device is constrained by the physical limits of the *X* and *Y* axes, which are defined by the boundaries of the beaker. Since the motion dynamics of the device exhibit a chaotic nature, the movement constraints are represented as X_c and Y_c. By leveraging chaotic motion, the stir bar effectively rotates at various points within the beaker, thereby increasing mixture homogeneity. To ensure that the system operates safely and precisely, limit switches are installed at the endpoints of the *X* and *Y* axes. These switches prevent the device from exceeding its designated workspace, thereby improving positioning accuracy and minimizing potential mechanical wear. The solid model and components of the developed device are illustrated in Fig. 5.

The designed system allows the magnetic stir bar to perform the mixing process not only from a fixed point but also at various positions by adjusting the beaker's location. The ability of the stir bar to change position ensures that the mixing process is not confined to a specific region but is instead evenly distributed throughout the entire mixture. As a result, higher mixing efficiency is expected than that of conventional fixed-point stirrers. Significant improvements in parameters such as homogeneity, pH balance, conductivity, and dissolution rate are anticipated.

The motion of the Cartesian platform is determined by the angular velocities (ω_{s1} and ω_{s2}) and rotational directions of the stepper motors. The mechanical design employed in this study enables independent control of the two stepper motors, allowing movement along the *X* and *Y* axes. The stepper motors operate in two rotational directions: CW (clockwise) and CCW (counterclockwise), with the platform's movement direction determined accordingly. Table 1 presents the relationship between the motor rotation directions and the corresponding motion of the platform in the Cartesian coordinate system.

Fig. 4 Cartesian platform design

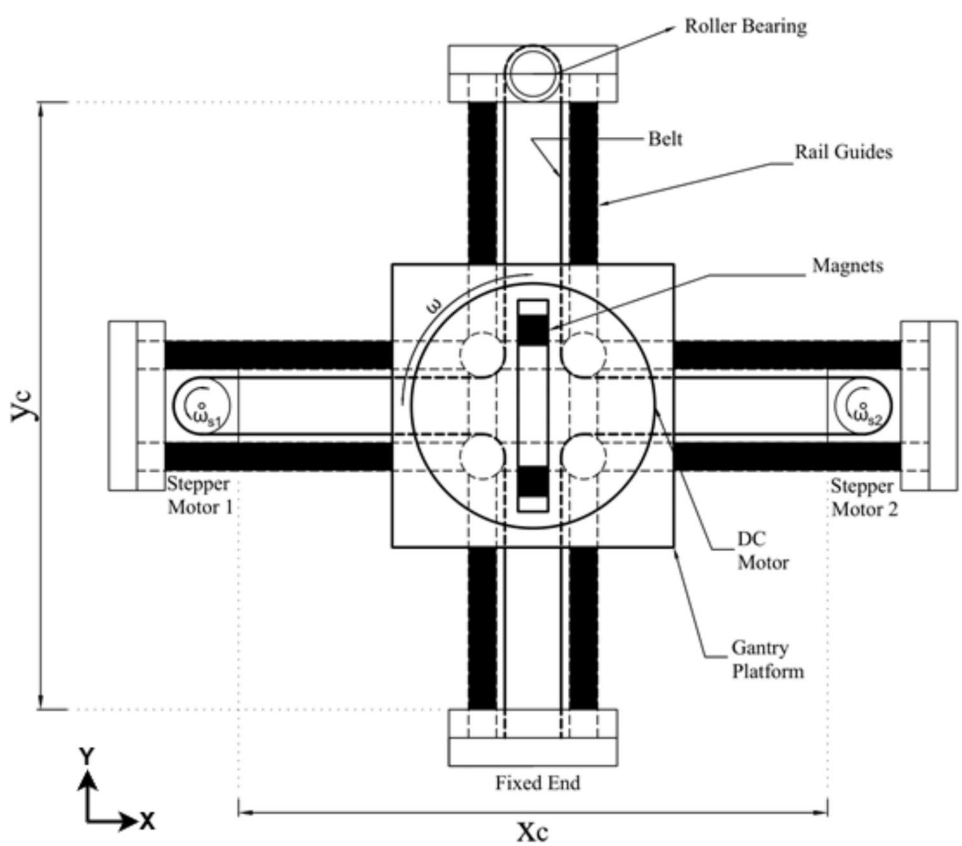

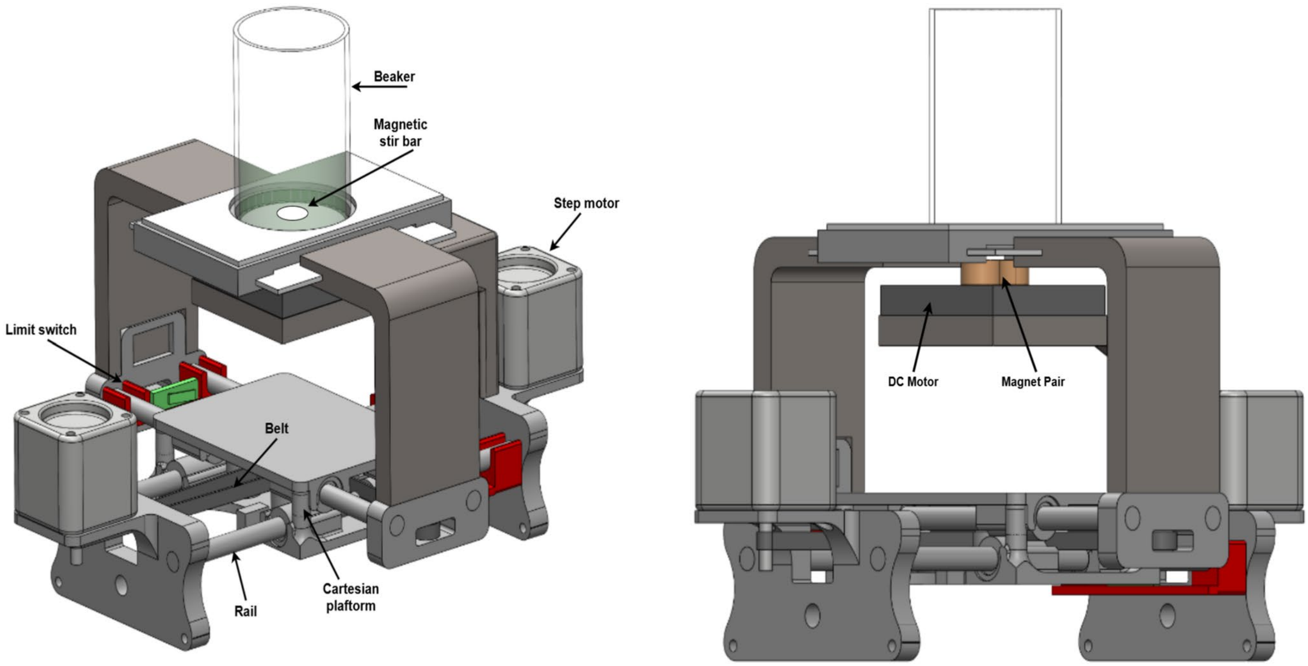

Fig. 5 Solid model of the developed device and components

Table 1 Axial motion configuration of the cartesian platform

ω_{s1} / ω_{s2}	CW	CCW
CW	←	↓
CCW	↑	→

The flowchart presented in Fig. 6 illustrates the operational sequence of the magnetic stirrer device, which integrates the chaotic positional changes of the magnetic stir bar. The process begins with the "start" step after the initial system parameters have been set. Following this, in the "determining the home position" phase, the stepper motors move the Cartesian platform via the belt mechanism until they reach the limit switches, thereby resetting the position data. This step ensures that the device precisely establishes its initial reference position, eliminating potential positioning errors. Once the platform reaches the designated position for the mixing process, the system proceeds to the next step. In the "start mixing" phase, the DC motor is activated, causing rotation of the magnet, which generates a magnetic field. This magnetic field induces the movement of the magnetic stir bar inside the beaker, thereby initiating the mixing process.

In the "Update Position Chaotically" phase, which constitutes a core innovation of the developed system, position data are generated by numerically solving well-known chaotic differential equations (Halvorsen, Sprott-A, and Lorenz systems) under predetermined initial conditions. The resulting time-dependent outputs for the x and y coordinates are scaled to ensure they remain within the geometric boundaries of the beaker's base area. These scaled values are then embedded into the memory of a single-board computer, which functions as the central control unit for real-time motion execution. The position data along the x and y axes, obtained from the numerical solutions of the selected chaotic system, are individually transmitted to two stepper motors that govern the movement of the Cartesian platform. Specifically, the x axis values control the first motor, while the y axis values are assigned to the second. This coordinated actuation enables the platform to reproduce the two-dimensional projection of the chaotic attractor in real physical space. As the stepper motors respond to these temporally evolving inputs, the beaker affixed to the platform undergoes continuous displacement governed by the nonlinear dynamics of the chaotic trajectory. Beneath the platform, a fixed magnet (mechanically coupled to a DC motor) remains stationary. However, as the beaker's position continuously changes in response to the chaotic motion model, the location of the magnetic stir bar within the solution also shifts. The stir bar remains magnetically coupled to the rotating magnet, and as its position within the beaker varies, it generates vortices that extend into previously stagnant or poorly mixed regions, particularly those along the beaker walls. This dynamic repositioning of the vortex source leads to more effective disruption of boundary-layer dead zones and improved suspension of undissolved particles. As a result, the system significantly enhances mixing efficiency and

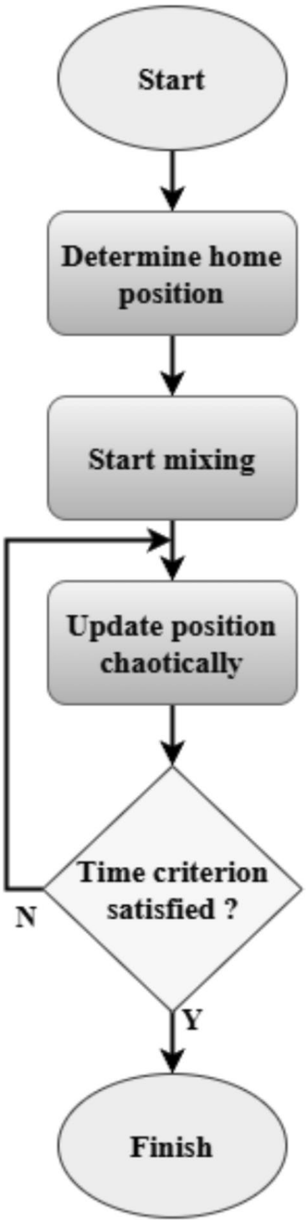

Fig. 6 Hardware flowchart

accelerates the transition to a homogeneous solution compared to conventional stirring devices, in which the stir bar remains fixed relative to the fluid container. When the process reaches the "time criterion satisfied?" decision point, the system checks whether the predefined mixing duration has elapsed. If the condition is not met ("N"), the chaotic position update loop continues, maintaining the active stirring process. Conversely, once the time limit is reached ("Y"), the system exits the loop and proceeds to the "Finish" step, thereby concluding the operational cycle of the device.

This approach leverages the inherent unpredictability and spatial complexity of chaotic motion to enhance mixing uniformity. Particularly effective in laboratory-scale processes involving low-viscosity solvents or solutes with intrinsically slow dissolution kinetics conditions that pose significant challenges to achieving rapid and homogeneous mixing. In such contexts, the dynamic and non-repetitive repositioning of the vortex-inducing region enables frequent disruption of peripheral zones and areas with limited fluid motion. This continuous spatial modulation strengthens convective transport mechanisms within the medium, facilitating more uniform solute dispersion across the entire fluid volume. As a result, the system not only accelerates the homogenization process but also ensures more complete and consistent dissolution, ultimately improving the efficiency, reliability, and reproducibility of physicochemical experiments.

In this study, the Mathematical Particle Tracing module of COMSOL Multiphysics was utilized to investigate the mixing effectiveness of the Halvorsen, Sprott-A, and Lorenz chaotic systems. Each system was appropriately scaled to fit the computational domain, and massless particles were released at $t=0$ to track their trajectories over time. For each system, the initial positions of a fixed number of particles were set within specific intervals based on the system's initial conditions. The velocities of these particles were determined by the variables of the corresponding chaotic system in each simulations. These particles formed the phase space for each system, enabling a visual examination of vortex formation, development, and trajectories.

The results presented in Fig. 7 demonstrate that the particles follow irregular and complex trajectories for each chaotic system at $t=50$ s. Among the systems analyzed, the Halvorsen system exhibits the densest and most uniform phase-space coverage. This superior performance can be attributed to the continuous, highly variable, and non-repetitive spatial motion generated by the Halvorsen attractor. Such dynamic behavior promotes the formation of vortex structures at varying locations within the beaker, effectively disrupting stagnant regions and enhancing overall fluid mixing. In comparison, the pseudo-symmetric Sprott-A system and the Lorenz system also generate chaotic trajectories; however, their spatial coverage is relatively less dense and exhibits more localized clustering. These differences highlight the particular advantage of the Halvorsen system in achieving widespread and uniform mixing dynamics, which is critical for reducing mixing time and increasing homogenization efficiency.

The analysis conducted in this study highlights the influence of chaotic dynamics on mixing behavior through particle trajectory evaluation. It should be emphasized that the structure of phase portraits is inherently

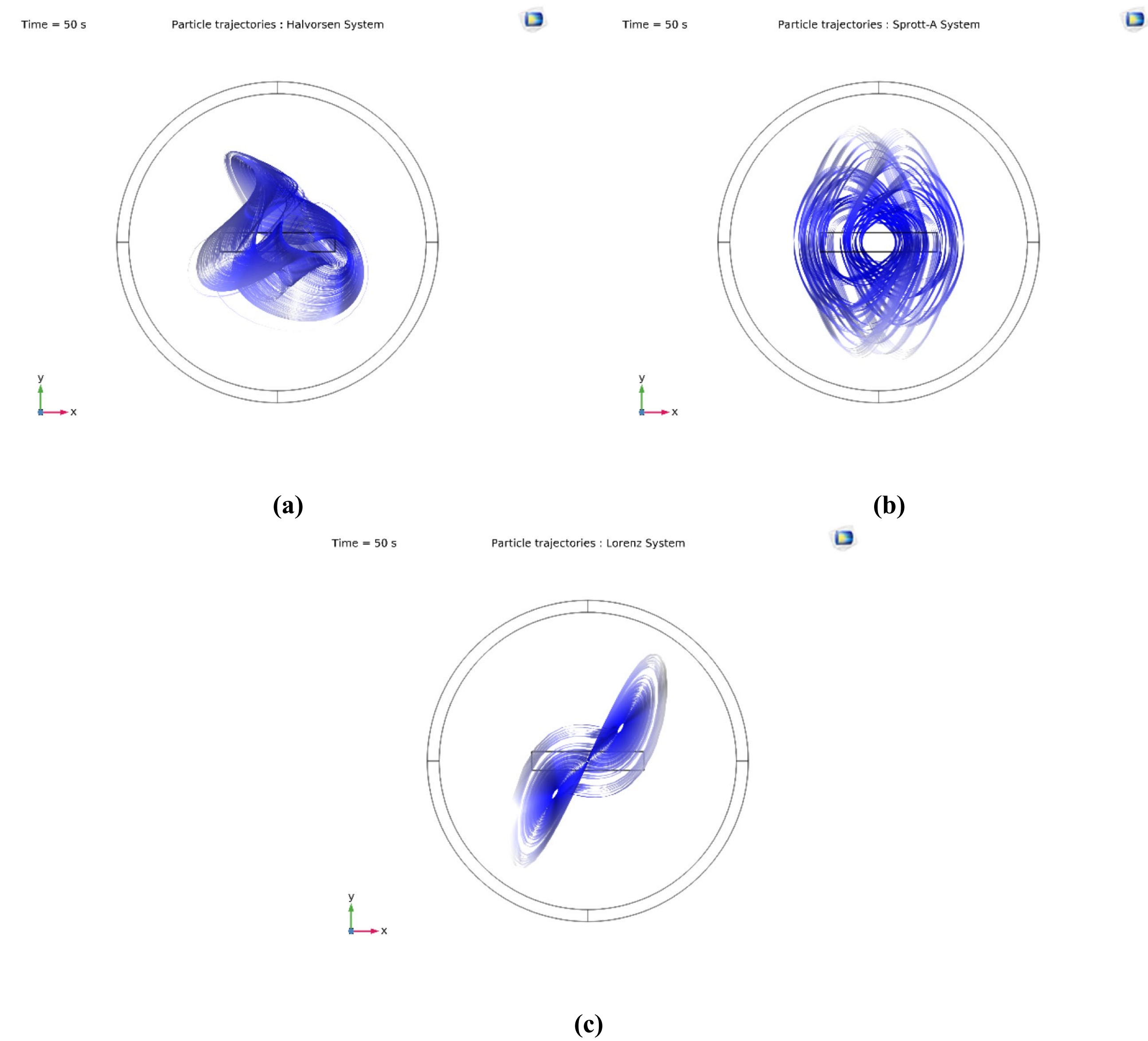

Fig. 7 Particle Tracing results for **a** Halvorsen, **b** Sprott-A and **c** Lorenz chaotic systems

dependent on the selection of variables plotted along the *x* and *y* axes for each chaotic system. Varying these variable pairings can lead to different trajectory topologies, which may influence the spatial distribution and transport of particles within the fluid domain. In conclusion, the particle tracking analysis conducted in this study clearly demonstrates the effective mixing behavior of chaotic systems and supports the validity of the proposed modeling approach.

This flowchart outlines an optimized method that improves the mixing time by dynamically changing the position of the magnetic stir bar based on chaotic motion principles. Algorithm 1 shows the pseudo-code of the system.

Algorithm 1 Pseudo-code of the system

```
Start
Select: chaotic system
Input: mixing_speed
Input: time_criterion
while limit_switch1 == 1 and limit_switch2 == 1 do
    Run stepper motors
end while
Move Gantry platform to (0,0) home position
Run DC motor at selected speed
time=0
while time<time criterion do
    Update gantry platform position chaotically
    Time=time+Δt // Update time based on system clock
end while
Stop DC motor and stepper motors
Finish
```

2.3 Experimental setup

In this study, the dissolution performance of a custom-designed prototype magnetic stirrer incorporating three distinct chaotic models (Halvorsen, Lorenz, and Sprott-A) was experimentally evaluated and compared with that of a conventional magnetic stirrer (Witeg, Germany). All experiments were conducted at room temperature (23 °C) using a 100 mL glass beaker with a base diameter of 50 mm. The allowable displacement range for the magnetic stir bar was constrained to ± 20 mm along both the X and Y axes within the beaker base. The DC motor speed was maintained at a constant 800 RPM in both the developed device and the conventional system. Chaotic motion trajectories were generated by numerically solving the chaotically equations corresponding to each chaotic system (Eqs. 1–3). The resulting X and Y axis position data were scaled to fit within the physical constraints of the beaker and transmitted to two independent stepper motors, allowing the Cartesian platform to reposition the beaker in real time according to the chaotic attractor dynamics. As the beaker moved along the chaotic orbit, the magnetic stir bar inside the solution produced a vortex that changed position over time. This dynamic repositioning enabled the stir bar to actively disturb fluid regions near the beaker walls, thus enhancing convective transport and accelerating the dissolution process. Each test involved preparing a solution of 80 mL deionized (DI) water and 0.25 g benzoic acid (Merck). Conductivity and pH values were recorded at predefined time intervals using an Isolab pH meter to monitor the dissolution progress. All measurements were repeated five times, and average values were used to ensure accuracy and reproducibility. The collected data were analyzed to assess and compare the efficiency of the chaotic stirring models with the conventional stirring method. The device used in the experimental process is shown in Fig. 8.

To quantitatively evaluate the performance enhancement offered by chaotic stirring systems over conventional magnetic stirrers, this study employed a comparative analysis based on the Area Under the Curve (AUC) methodology. Specifically, AUC values were computed for the conductivity-time and pH-time response curves obtained during the mixing processes of both stirring systems. The AUC represents a numerical approximation of the definite integral of a function over a specified time interval and is frequently utilized to evaluate cumulative effects or total responses in dynamic systems, including chemical mixing, pharmacokinetics, and environmental monitoring [62, 63]. In this context, the trapezoidal rule (a widely adopted numerical integration method) was applied to estimate the AUC for each curve. This method segments the curve into a series of adjacent trapezoids and sums their areas to yield an accurate approximation of the integral. The use of AUC allows for a holistic comparison of time-dependent behaviors by capturing the total conductivity or pH change throughout the entire mixing duration, rather than relying solely on instantaneous or peak values.

The percentage improvement of each chaotic model over the conventional stirrer was computed via Eq. (4).

$$\%\ \text{Efficiency} = \frac{AUC_{chao} - AUC_{conv}}{AUC_{conv}} \times 100 \tag{4}$$

Here, AUC_{chao} and AUC_{conv} denote the cumulative integrals for the chaotic and conventional stirrers, respectively, based on the measured parameters. This formulation provides a normalized efficiency metric, facilitating direct comparison across different mixing trials and conditions.

The AUC approach has been extensively applied in prior studies to assess mixing efficiency and system dynamics. For instance, in biochemical engineering, it has been used to evaluate substrate conversion rates and enzyme activity over time [64]; in environmental systems, AUC aids in monitoring pollutant dispersion or nutrient mixing [65]. The incorporation of AUC in this study enables a robust and interpretable framework for benchmarking chaotic mixing against traditional stirring techniques.

3 Results and discussion

Conductivity-time and pH-time data were first analyzed to assess the mixing efficiency of the chaotic stirrers in comparison with the conventional method. The detailed measurement results supporting this analysis are provided in the supplementary materials (Supplementary Tables S1–S4),

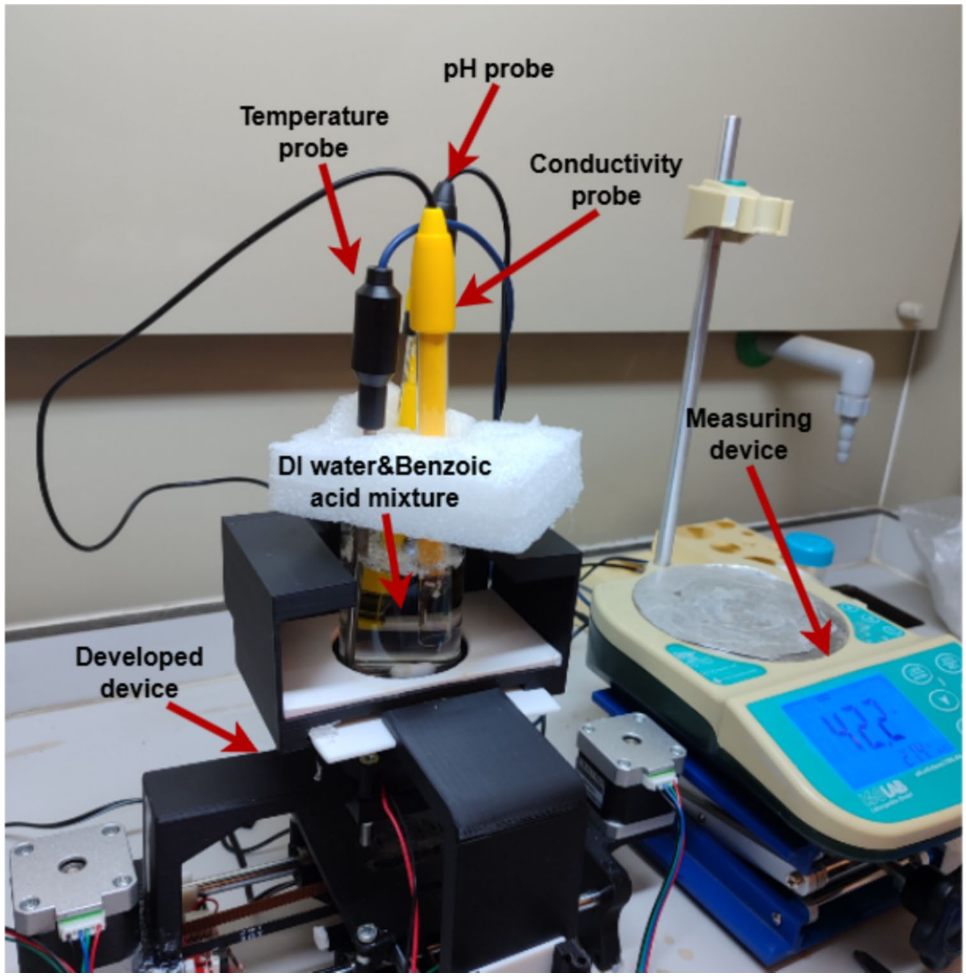

Fig. 8 Experimental test (DI water and benzoic acid mixture)

which include both short- and long-term values across all stirring models.

In this study, two distinct experimental protocols were employed to assess the mixing performance of various stirring strategies. The first set of experiments focused on short-term mixing behavior, evaluating conductivity and pH responses over a 15 min period to determine the rate and extent of solute incorporation at early stages of mixed. The second set of experiments was designed to investigate long-term mixing dynamics, where in the time required for each method to reach solution saturation was systematically recorded. This approach enabled a comparative evaluation of each stirring method's effectiveness in achieving complete solute dissolution over extended durations. Short-term experiments, the Halvorsen chaotic model attained the highest conductivity and the lowest pH value at the 15 min time. This outcome is not coincidental but rather a direct consequence of the mathematical structure of the Halvorsen system, which incorporates exponential terms that induce high sensitivity to initial conditions and promote broader, non-repetitive phase-space traversal. This continuous and non-repeating motion translates into more dynamic repositioning of the magnetic stirrer (magnetic stir bar), leading to the formation of transient, shifting vortices throughout the fluid domain. This behavior has a profound effect on the mixing process. As the position of the magnetic stir bar varies, so too does the location of vortex formation, minimizing the likelihood of persistent dead zones (particularly near the beaker walls) where undissolved materials often accumulate in conventional systems. In contrast to traditional setups, where the vortex is fixed and dissolution occurs slowly due to limited convective transport, the Halvorsen model continuously disrupts these stagnant regions, pulling insoluble particles from the surface and periphery into the active flow field, thereby accelerating solute incorporation.

As shown in Fig. 9a and detailed in Table 2, the Halvorsen model achieved the highest short-term conductivity with an AUC value of 3068.43 μS·min, corresponding to an improvement of 11.99% over the conventional stirrer (2739.83 μS·min). This result indicates that the Halvorsen model facilitates faster solute dissolution and more efficient mixing dynamics. The Sprott-A model also exhibited improved performance, with a 4.21% higher AUC than the conventional method. In contrast, the Lorenz model showed

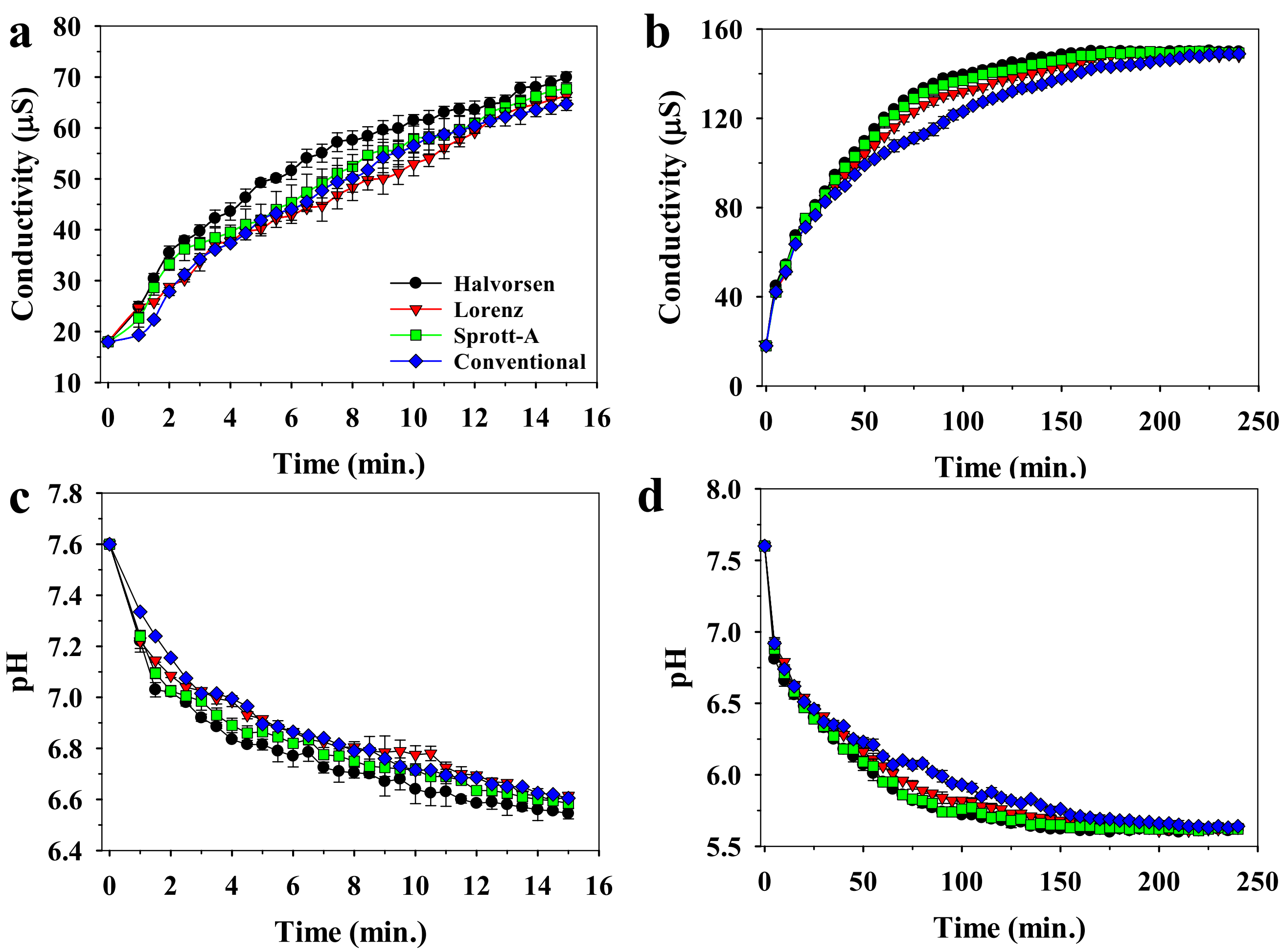

Fig. 9 Time-dependent conductivity and pH for chaotic (Halvorsen, Lorentz, Sprott-A) and conventional stirrers: **a** short-term conductivity, **b** long-term conductivity, **c** short-term pH, **d** long-term pH

Table 2 AUC values and percentage differences in short- and long-term conductivity for different stirring methods

Model	Short-term		Long-term	
	AUC (µS·min)	%Difference in conductivity	AUC (µS ·min)	%Difference in conductivity
Halvorsen	3068.43	11.99	1239.66	7.70
Lorenz	2695.15	– 1.63	1197.66	4.05
Sprott-A	2855.23	4.21	1225.71	6.48
Conventional	2739.83	–	1151.09	–

a slight underperformance with an AUC 1.63% lower than that of the conventional approach.

The long-term conductivity behavior, presented in Fig. 9b and Table 2, reveals how each method performs over extended mixing durations. While all models eventually reached a conductivity plateau, the Halvorsen model again proved most effective, achieving a long-term AUC of 1239.66 µS·min. This represents a 7.70% improvement compared to the conventional stirrer's AUC of 1151.09 µS·min. The Sprott-A model followed with a 6.48% increase, and the Lorenz model reached 1197.66 µS·min, corresponding to a 4.05% improvement. These results confirm that the superior performance of the Halvorsen model is sustained over time, highlighting its robustness in enhancing dissolution efficiency.

In long-term conductivity evaluations, the Halvorsen model demonstrated superior performance by reaching the saturation point at the 150th minute, indicating that the solution had attained its maximum solute concentration. This outcome further substantiates the effectiveness of the Halvorsen system's intricate flow dynamics and broad spatial influence in accelerating mass transfer and promoting comprehensive solute dissolution.

The Sprott-A model reached the saturation point at approximately the 160th minute, thereby ranking as the second most effective chaotic configuration in long-term mixing performance. Although its phase-space representation exhibits considerable spatial coverage, it lacks the high-density, multidirectional divergence observed in the Halvorsen system. As a result, although the Sprott-A attractor exhibits slightly lower trajectory traversal density and frequency compared to the Halvorsen system, it nonetheless achieves effective mixing across the fluid domain, with only a modest delay in reaching solution saturation thereby demonstrating its competence as a viable chaotic mixing strategy.

The Lorenz model, on the other hand, reached saturation at around the 175th minute. Its phase portrait exhibits symmetrical, butterfly-shaped attractors that offer more predictable and repetitive trajectories. This symmetry inherently limits the spatial variability of the magnetic stir bar's movement, resulting in lower frequency interaction with stagnant boundary layers. Consequently, undissolved material in beaker dead zones remains unperturbed for longer durations compared to the Halvorsen and Sprott-A models.

The conventional magnetic stirring method exhibited markedly inferior performance compared to all chaotic configurations, with solution saturation only occurring around the 215th minute. This deficiency is primarily attributed to the fixed, centrally rotating magnetic stir bar, which generates a limited vortex confined to the center of the beaker. Consequently, insolutes located along the beaker walls or floating at the surface remain largely unaffected by the central vortex and are inefficiently incorporated into the bulk mixture. The absence of spatial modulation in conventional stirring significantly hinder the disruption of dead zones, especially in low-viscosity media with inherently slow dissolution kinetics. These findings indicate that conventional magnetic stirrers prolong the time it takes to achieve mixture homogeneity under these conditions. The graph showing the time-dependent saturation of the solutions according to different mixing methods in the long-term mixing experiment is shown in Fig. 10.

In terms of pH behavior, Fig. 9c and Table 3 illustrate the short-term process. A lower AUC in the pH-time curve indicates a quicker transition to equilibrium. The Halvorsen stirrer reached the lowest short-term pH AUC value of 384.72 pH·min, reflecting a 1.40% improvement over the conventional method (390.18 pH·min). The Sprott-A model also showed improvement with a 0.70% reduction, while the Lorenz model remained nearly identical to the conventional stirrer, with a marginal 0.06% decrease. These results demonstrate that chaotic stirring enhances not only conductivity but also the speed of reaching pH stability, particularly with the Halvorsen configuration.

The long-term pH stabilization is presented in Fig. 9d and summarized in Table 3. Over extended mixing periods, the

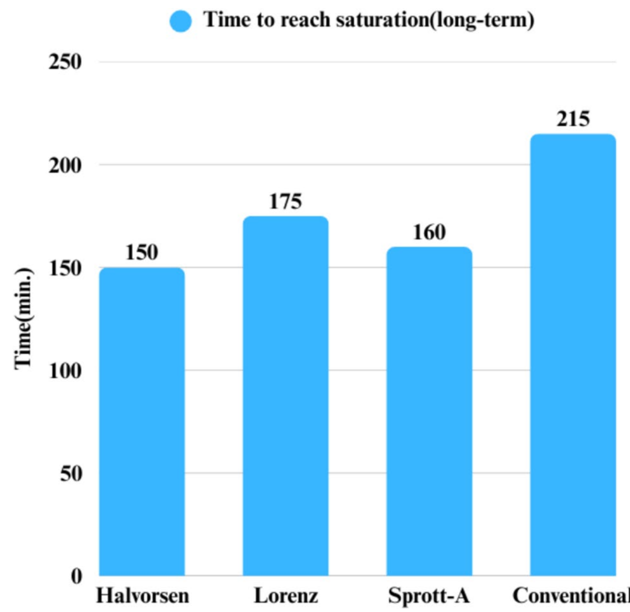

Fig. 10 Time for solution to reach saturation (long-term)

Halvorsen model continued to provide the fastest stabilization with a pH AUC of 56.176 pH·min, which is 1.98% lower than the conventional stirrer's AUC of 57.308 pH·min. The Sprott-A and Lorenz models recorded reductions of 1.68% and 0.98%, respectively. This consistent reduction in AUC across both short- and long-term measurements emphasizes the effectiveness of chaotic stirring, particularly the Halvorsen model, in promoting rapid chemical equilibrium during dissolution.

The overall performance comparison of all stirring methods is visually summarized in Fig. 11, which presents both short-term and long-term percentage differences in conductivity and pH. The Halvorsen model consistently demonstrates the highest performance gains across both parameters and time scales, confirming its superior stirring dynamics. The Sprott-A model exhibits moderate yet stable improvements, while the Lorenz model provides more modest benefits compared to the conventional stirrer. These findings clearly show that among the tested chaotic models, Halvorsen delivers the most balanced and effective performance in enhancing both dissolution rate and chemical stability. This superior performance of the Halvorsen model can be attributed to its strongly dissipative but bounded chaotic attractor, which provides multi-dimensional phase-space coverage with minimal periodicity. Unlike Lorenz, which exhibits symmetry and saddle-type instabilities, or Sprott-A, which has a simpler structure, the Halvorsen system continuously generates new, non-repeating trajectories that allow for better fluid particle dispersion over time.

The findings of this study reinforce the growing consensus that chaotic mixing strategies, particularly those governed by

Table 3 AUC values and percentage differences in short- and long-term pH for different stirring methods

Model	Short-term		Long-term	
	AUC (pH·min)	%Difference in pH	AUC (pH·min)	%Difference in pH
Halvorsen	384.715	−1.40	56.176	−1.98
Lorenz	389.925	−0.06	56.749	−0.98
Sprott-A	387.435	−0.70	56.346	−1.68
Conventional	390.178	–	57.308	–

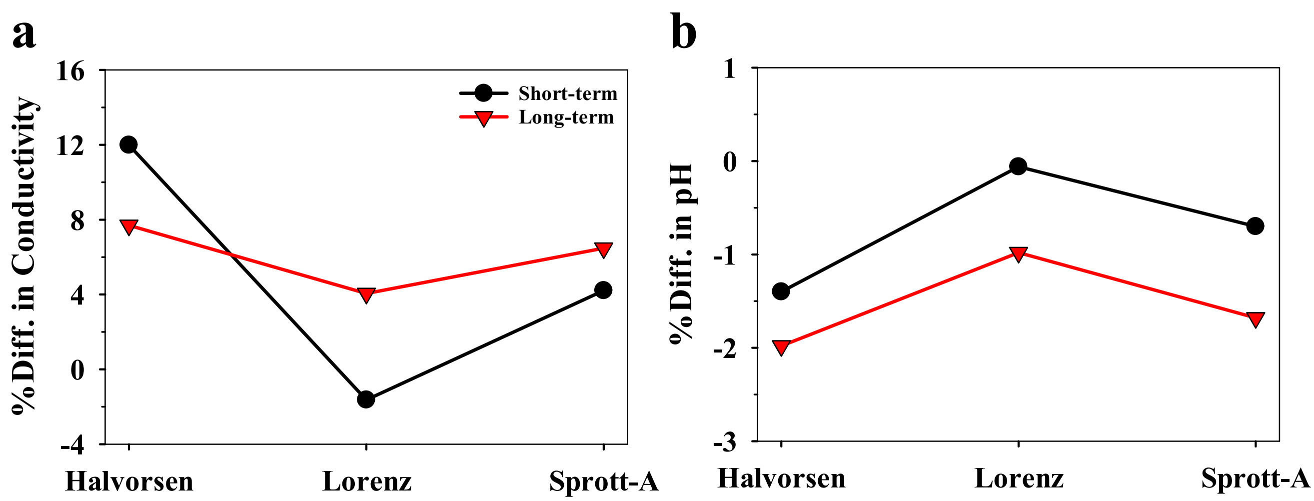

Fig. 11 AUC-based percentage differences of chaotic and conventional stirring methods for **a** conductivity and **b** pH in short- and long-term measurements

the dynamics of nonlinear attractors, offer significant advantages over conventional mixing techniques especially in low-viscosity environments with slow dissolution kinetics. Among the systems evaluated, the Halvorsen model demonstrated the highest spatial coverage and temporal variability, leading to effective disruption of stagnation zones near the vessel walls and the solution surface. These regions, often inaccessible to traditional magnetic stirrers with fixed central axes, were efficiently engaged through the reorienting and volumetrically extensive vortex structures induced by chaotic motion. This observation is supported by literature indicating that irregular, non-repetitive motion patterns (whether in the form of chaotic spatial trajectories or speed variations) prevent the formation of consistent flow paths, thus minimizing unmixed regions within the medium [21, 23, 66–68]. Experimental comparisons further reveal that chaotic trajectories at constant speed outperform fixed-position mixing at the same speed in terms of homogeneity [66]. Moreover, the introduction of chaos into the rotational speed of DC motors, as explored using various attractor systems (e.g., Chua, Newton–Leipnik, Lorenz, Rössler), not only improves mixing uniformity but also reduces energy consumption. Specifically, studies identified the Chua and Hadley systems as yielding lower average power and energy usage compared to other chaotic signals, highlighting their potential for energy-efficient mixing operations [66, 68].

These results align with broader literature demonstrating that chaotic strategies (especially those utilizing variable positioning, nonlinear trajectories, and frequency modulation) consistently outperform laminar or turbulent approaches across diverse domains, from microfluidics to polymer blending [20–25, 28–34, 39, 41–44]. Advanced implementations such as robotic stirrer platforms and fractal impellers have also been shown to enhance dispersion and shorten processing durations through vortex modulation and adaptive flow reorientation [26, 33, 44]. Nevertheless, the effectiveness of chaotic stirring is not universal and must be contextualized within the specific fluidic and geometric parameters of the system. Factors such as solute particle size, mixer tip design, container dimensions, and the rheological properties of the medium significantly influence outcomes [21, 38–40].

The superior performance of the Halvorsen chaotic system in enhancing mixing efficiency can be theoretically explained by examining the geometric and dynamic properties of its system. Unlike the Lorenz and Sprott-A systems, which often exhibit more structured and symmetric trajectories, the Halvorsen system displays a more diffused, three-dimensional swirl-like structure that covers a broader area in phase space. This allows for greater spatial variability and randomness in the stir bar's trajectory, effectively increasing the turbulence intensity and minimizing the formation of stagnation zones during mixing. Such widespread chaotic systems induce stronger sensitivity to initial conditions and non-repetitive orbital transitions, which are beneficial for maximizing contact between solute and solvent. Furthermore, the Halvorsen system includes nonlinear damping terms (e.g., $-y^2$, $-z^2$) in its state equations, which generate more abrupt trajectory shifts and lead to localized high-gradient zones in the position field. This contributes to a higher degree of mixing randomness compared to the smoother flow fields of Lorenz or Sprott-A systems. As chaotic mixing relies heavily on Lagrangian particle stretching and folding, the geometrical complexity and temporal irregularity of Halvorsen dynamics make it particularly suitable for enhanced dispersion in fluid systems. This theoretical rationale is consistent with the observed increase in conductivity and faster pH stabilization in the experimental results.

4 Conclusion

This study conducted a comparative analysis of the dissolution efficiency of three chaotic stirring models (Halvorsen, Sprott-A, and Lorenz) against a conventional magnetic stirring system. In contrast to the fixed, circular motion of conventional stir bars, the chaotic configurations employed non-repetitive trajectories derived from deterministic chaotic attractors, enabling continuous spatial repositioning of the stir bar. This dynamic movement generated time-varying vortex patterns within the fluid, actively disturbing low-flow regions and enhancing solute transport throughout the medium. Among the chaotic models, the Halvorsen system demonstrated the highest performance, achieving superior conductivity values and the most rapid pH stabilization. Its spatially unpredictable and temporally continuous motion facilitated more effective mixing by improving vortex coverage and minimizing dead zones. The Sprott-A model also outperformed the conventional approach, confirming the general benefit of chaotic motion for solute dispersion. In contrast, the Lorenz model exhibited slightly lower efficiency, likely due to its symmetrical phase portrait and more limited spatial excitation. pH data supported these findings, as Halvorsen and Sprott-A models both showed lower AUC values, reflecting quicker stabilization. Complementary to these dissolution and pH measurements, a particle tracing analysis was conducted to further investigate the influence of chaotic dynamics on mixing behavior. The results presented in the particles follow irregular and complex trajectories for each chaotic system at. Among the systems analyzed, the Halvorsen system exhibited the densest and most uniform phase-space coverage. This superior performance can be attributed to the continuous, highly variable, and non-repetitive spatial motion generated by the Halvorsen attractor. Such dynamic behavior promotes the formation of vortex structures at varying locations within the beaker, effectively disrupting stagnant regions and enhancing overall fluid mixing. In comparison, the pseudo-symmetric Sprott-A system and the Lorenz system also generated chaotic trajectories; however, their spatial coverage was relatively less dense and exhibited more localized clustering. These differences further highlight the particular advantage of the Halvorsen system in achieving widespread and uniform mixing dynamics, which is critical for reducing mixing time and increasing homogenization efficiency. Based on the experimental findings and particle tracking analyses, it can be concluded that the Halvorsen model provides the most effective approach for achieving fast and uniform mixing. Its position-based control of the magnetic stir bar offers both precision and energy efficiency, making it particularly suitable for applications in chemical processing, biological systems, and pharmaceutical production.

Future studies will focus on regulating the speed variations of the DC motor chaotically to investigate its impact on mixture homogeneity. Additionally, the conventional open-loop heating process in traditional stirrers is replaced with a feedback-based closed-loop system to increase the mixing efficiency. Finally, an Internet of Things (IoT)-based application is developed for remote data collection and analysis, enabling real-time monitoring and optimization.

Supplementary Information The online version contains supplementary material available at https://doi.org/10.1007/s40430-025-05840-2.

Acknowledgements This research was supported by Turkish Research Council (Project No:124M843).

Data availability The authors have no competing interests to declare that are relevant to the content of this article. All the data generated or analyzed during this study are included in this published article.

References

1. Ibadillah A, Alfita R, Laksono DT (2021) Hotplace magnetic stirrer automatic heat control and water velocity based on PID (Proportional integral derivative). Proc Eng Life Sci 1(1):766
2. Soesilo D, Rizal M (2021) Invitro micro encapsulation of beta tri calcium phosphate from anadara granosa shell synthesis. Denta 14(2):71–76. https://doi.org/10.30649/denta.v14i2.3
3. Ariessaputra S, Putra MA (2023) Rancang bangun hot plate magnetic stirrer berbasis mikrokontroler. Dielektrika 10(2):195–202
4. Schneider S, Seidel S, Seefeldt A, Romang M, Kastl S, Gensel J, Eibl D (2023) 3d printed, single-use bioreactor with integrated inline sensors for microbial and mammalian cell cultivation—a case study. Processes 11(11):3231. https://doi.org/10.3390/pr11113231
5. Nurhidayati D (2024) Laboratory scale of rayon fiber manufacturing: manual stirring and stirring using a magnetic stirrer. Berkala Penelitian Teknologi Kulit, Sepatu, dan Produk Kulit 23(1):7–12
6. Halász G, Gyüre B, Jánosi IM, Szabó KG, Tél T (2007) Vortex flow generated by a magnetic stirrer. Am J Phys 75(12):1092–1098
7. Mataram A, Nasution S, Wijaya ML, Septano GD (2017) Physical and mechanical properties of membrane Polyacrylonitrile. In: MATEC web of conferences. EDP sciences, Vol. 101, pp 01010

8. Kuśmierek K, Świątkowski A (2015) The influence of different agitation techniques on the adsorption kinetics of 4-chlorophenol on granular activated carbon. React Kinet Mech Catal 116:261–271
9. Subratti A, Lalgee LJ, Jalsa NK (2019) Robust, efficient, and economical magnetic stirrer: a device based on pulsed width modulation, built using mainly recycled parts. J Chem Educ 97(1):305–307
10. Nugraha IMA, Mahardiananta IMA, Putra PAM, Adnyana IGS (2022) Magnetic stirrer with speed advisor and timer based on microcontroller. J Robot Control (JRC) 3(1):18–25
11. Langrish TA, Zhong C, Sun L (2021) Probing differences in mass-transfer coefficients in beaker and stirrer digestion systems and the USP dissolution apparatus 2 using benzoic acid tablets. Processes 9(12):2168
12. Tohidi B, Burgass RW, Danesh A, Østergaard KK, Todd AC (2000) Improving the accuracy of gas hydrate dissociation point measurements. Ann N Y Acad Sci 912(1):924–931
13. Zha Z, Ye Z (2022) Numerical study of unsteady shock/mixing interaction in confined space. Proc Inst Mech Eng Part G: J Aerospace Eng 236(8):1667–1677
14. Hsu CW, Shih PT, Chen JM (2020) Enhancement of fluid mixing with U-shaped channels on a rotating disc. Micromachines 11(12):1110
15. Rezaeian M, Nouri M, Hassani-Gangaraj M, Shamloo A, Nasiri R (2022) The effect of non-uniform magnetic field on the efficiency of mixing in droplet-based microfluidics: a numerical investigation. Micromachines 13(10):1661
16 Susilo SH, Asrori A (2021) Analysis of position and rotation direction of double stirrer on chaotic advection behavior. EUREKA Phys Eng 2:78–86
17. Campbell GA, Taylor R, Wetzel MD, Chempath S, Bomma S, St. John S, Powers DL (2022) Chaotic mixing in a free-helix extruder using a new solution to the biharmonic equation. AIChE J 68(4):e17557
18. Mishra SP (2021) Concentration effect of sodium chloride salt on benzoic acid solubility and dissociation into water at 298 K temperature. Int Res J Pure Appl Chem 22(6):47–52
19. Kitazoe K, Park YS, Kaji N, Okamoto Y, Tokeshi M, Kogure K, Baba Y (2012) Fabrication of functionalized double-lamellar multifunctional envelope-type nanodevices using a microfluidic chip with a chaotic mixer array. Plos one 7(6):e39057
20. Ji M, Wu Z, Ferrari A, Fu L, Vento O (2023) Experimental investigation on Gasoline—water mixture fuel impingement preparation method and spray characteristics with high injection temperatures and pressures. Energies 16(16):6026
21. Yagmur D, Kutlu M (2024) 3D chaotic mixing application for polymer production. Phys Scr 99(4):045210
22. Burghelea T, Segre E, Bar-Joseph I, Groisman A, Steinberg V (2004) Chaotic flow and efficient mixing in a microchannel with a polymer solution. Phys Rev E Statis, Nonlinear, Soft Matter Phys 69(6):066305
23. Kalayci O, Pehlivan I, Akgul A, Coskun S, Kurt E (2021) A new chaotic mixer design based on the Delta robot and its experimental studies. Math Probl Eng 2021(1):6615856
24. TabkhPaz M, Mahmoodi M, Arjmand M, Sundararaj U, Chu J, Park SS (2015) Investigation of chaotic mixing for MWCNT/polymer composites. Macromol Mater Eng 300(5):482–496
25 Matos J, Santos RJ, Dias MM, Lopes JCB (2024) Chaos and mixing in NETmix. AIChE J 2024:e18461
26. Robinson M, Cleary PW (2011) The influence of cam geometry and operating conditions on chaotic mixing of viscous fluids in a twin cam mixer. AIChE J 57(3):581–598
27. He Y, Zhan X, Shen B, Sun Z, Long J, Yang Y, Li X (2022) Chaotic advection in a twin cam mixer under various operating conditions. AIChE J 68(2):e17492
28. Akay S, Kayan B, Peña MÁ, Jouyban A, Martínez F, Acree WE Jr (2022) Expanding the equilibrium solubility and dissolution thermodynamics of benzoic acid in aqueous alcoholic mixtures. Reactions 3(3):392–414
29. Liu B, Sun N, Jin Z, Zhang Y, Sunden B (2019) Numerical investigation and estimating correlation of micromixing performance of coaxial mixers. Ind Eng Chem Res 58(49):22376–22388
30. Wang J, Huang Y, Zhang R, Zhou L (2024) Numerical and experimental study of homogenization mechanism of high shear rotor-stator mixer. Can J Chem Eng 102(12):4216–4229
31. Li Y, Wang S, Wang Q, Zhu M, Shan W, Liu Y (2023) CsCu 0.1 H 29 PMo 11 VO 40 catalyst synthesized via a high shear mixer facilitated precipitation method for selective oxidation of methacrolein to methacrylic acid. Catal Sci Technol 13(6):1874–1887
32. Yatsunov AN, Sabiev UK (2022) Comparative analysis of the working bodies of the vibrating mixer of bulk feed. Tractors Agric Mach 89(5):367–374
33 Andrzej M, Misztal W, Savinykh P, Turubanov N, Isupov A, Zyryanov D (2019) Improving efficiency of horizontal ribbon mixer by optimizing its constructional and operational parameters. Eksploatacja i Niezawodność 21(2):5
34. Christ R, Pacheco F, Ehrenbring HZ, Lopes RK, Tutikian BF, Funke GBN (2023) Effect of type of mixer on rheological and mechanical behavior of ultra high-performance concrete. Struct Concr 24(3):4276–4285
35. Wang Y, Zhang Y, Qiao Z, Wang W (2020) A 3D printed jet mixer for centrifugal microfluidic platforms. Micromachines 11(7):695
36 Kazemzadeh A (2016) Mixing of Complex Fluids with the Coaxial Mixers Composed of Two Central Impellers and an Anchor. Ryerson University, UK
37. Shanko ES, van de Burgt Y, Anderson PD, den Toonder JM (2019) Microfluidic magnetic mixing at low Reynolds numbers and in stagnant fluids. Micromachines 10(11):731
38. Yang K, Zhang X, Yang G, Li M, Wang H, Xiao Q (2024) Dynamic chaos of imaging measurements for characterizing gas–liquid nonlinear flow behaviour in a metallurgical reactor stirred by top-blown air. Can J Chem Eng 102(2):979–995
39. Velásquez-Parra A, Marone F, Griffa M, Jiménez-Martínez J (2024) Chaotic transport of solutes in unsaturated porous media. Environ Sci Technol 58(28):12643–12652
40. Bu F, Jiao Y, Wang J (2024) Novel close-clearance impeller structure for solid-liquid mixing at low Reynolds numbers based on the Paravisc impeller. Ind Eng Chem Res 63(35):15585–15599
41. Gu D, Mei Y, Wen L, Wang X, Liu Z (2021) Chaotic mixing and mass transfer characteristics of fractal impellers in gas-liquid stirred tank. J Taiwan Inst Chem Eng 121:20–28
42 Aquino T, Borgne TL, Heyman J (2023) Fluid–solid reaction in porous media as a chaotic restart process. Phys Rev Lett 130(26):264001. https://doi.org/10.1103/physrevlett.130.264001
43. Proskurina OGV, Sivtsov EV, Enikeeva MO, Sirotkin AA, Sh AR, Gusarov VV (2019) Formation of rhabdophane-structured lanthanum orthophosphate nanoparticles in an impinging-jets microreactor and rheological properties of sols based on them. Nanosyst Phys Chem Math 10(2):206–214
44. Gupta VK, Jha PK, Jain PK (2024) Numerical investigations of stirring induced flow on solidification and interface behavior in continuous casting mold with bifurcated nozzle. ASME J Heat Mass Transfer 146(6):062402
45. Tél T, Kadi L, Jánosi IM, Vincze M (2018) Experimental demonstration of the water-holding property of three-dimensional vortices. Europhys Lett 123(4):44001
46. Sidauruk AN, Amal MI, Marlianto E (2022) Effect of additional Cu on structural and optical properties of TiO_2 synthesized with sol-gel method. J Technomater Phys 4(1):54–62
47. Ibadillah AF, Rahmawati D, Elismawati E, Alfita R, Wibisono KA, Ulum M, Haryanto H, Ubaidillah A, Nahari RV (2018)

Designing magnetic stirrer hot plate using contactless infrared MLX90614 temperature sensor based on PID controller. In: International conference on science and technology (ICST 2018). Atlantis Press, pp 940–944
48. Shu Z, Zhu S, Zhang J, Zhao W, Ye Z (2020) Optimization design and analysis of polymer high efficiency mixer in offshore oil field. Processes 8(1):110
49 Strogatz SH (2001) Nonlinear dynamics and chaos: with applications to physics, biology, chemistry, and engineering (studies in nonlinearity). Westview Press, UK
50. Lorenz EN (1963) Deterministic nonperiodic flow. J Atmos Sci 20(2):130–141
51. Van der Pol B, Van Der Mark J (1927) Frequency demultiplication. Nature 120(3019):363–364
52. Kennedy M, Chua L (1986) Van der Pol and chaos. IEEE Trans Circ Syst 33(10):974–980
53 Kennedy MP (1995) Experimental chaos from autonomous electronic circuits. Philos Trans R Soc London Series A: Phys Eng Sci 353(1701):13–32
54 Lai YC, Tél T (2011) Transient chaos: complex dynamics on finite time scales. Springer Science & Business Media, UK
55. Hamida El Naser Y, Karayel D (2024) Modeling the effects of external oscillations on mucus clearance in obstructed airways. Biomech Model Mechanobiol 23(1):335–348
56. Kia B, Spano ML, Ditto WL (2011) Chaos computing in terms of periodic orbits. Phys Rev E Stat Nonlinear Soft Matter Phys 84(3):036207
57. Hilborn RC (2000) Chaos and nonlinear dynamics: an introduction for scientists and engineers. Oxford University Press
58 Wiggins S, Ottino JM (2004) Foundations of chaotic mixing. Philos Trans R Soc London Series A: Math Phys Eng Sci 362(1818):937–970
59. Sasmal C (2022) Fluid viscoelasticity suppresses chaotic convection and mixing due to electrokinetic instability. Phys Fluids 34(8):082011
60. Ye S, Chau KT (2007) Chaoization of DC motors for industrial mixing. IEEE Trans Ind Electron 54(4):2024–2032
61 Kurt E (2017) Yeni bir kaotik karıştırıcı tasarımı ve uygulaması. Sakarya Universitesi, Turkey
62. Horton AJ, Clayton SB (2020) Optimization of impedance-measured reflux events in GORD utilizing acid exposure time. BMC Gastroenterol 20:1–8
63. Reich K, Hansen JB, Puig L, Konstantinou MP, Warren RB (2021) Complete clearance and Psoriasis Area and Severity Index response for brodalumab and ustekinumab by previous treatment history in AMAGINE-2 and AMAGINE-3. J Eur Acad Dermatol Venereol 35(10):2034–2044
64. Jamshed A, Cooke M, Ren Z, Rodgers TL (2018) Gas–liquid mixing in dual agitated vessels in the heterogeneous regime. Chem Eng Res Des 133:55–69
65. Bekele E, Zhang Y, Donn M, McFarlane D (2019) Inferring groundwater dynamics in a coastal aquifer near wastewater infiltration ponds and shallow wetlands (Kwinana, Western Australia) using combined hydrochemical, isotopic and statistical approaches. J Hydrol 568:1055–1070
66. Sahin S, Kavur AE, Mustafov SD, Seydibeyoglu O, Baser O, Isler Y, Guzelis C (2020) Spatiotemporal chaotification of delta robot mixer for homogeneous graphene nanocomposite dispersing. Robot Auton Syst 134:103633
67. Honglad S, San-Um W (2014) Automatic stand-alone liquid mixer with chaotic PWM control using diode-based Rössler system. In: 2014 international electrical engineering congress (iEECON), IEEE, pp 1–4
68. Zhao Z, Jian J, Wang W (2012) Estimations of bounds and synchronization controlling for hadley chaotic system. In: 2012 IEEE international conference on information science and technology, IEEE, pp 150–152

Authors and Affiliations

Mert Süleyman Demirsoy[1] · Muhammed Salih Sarıkaya[1] · Sedat Kurnaz[2] · Yusuf Hamida El Naser[1] · Mehmet Ali Hazar[3] · Selçuk Coşkun[3] · Mustafa Çağrı Kutlu[1,4] · Gizem Hazar[3]

✉ Mert Süleyman Demirsoy
mertdemirsoy@subu.edu.tr

Muhammed Salih Sarıkaya
salihsarikaya@subu.edu.tr

Sedat Kurnaz
sedatkurnaz@kastamonu.edu.tr

Yusuf Hamida El Naser
yusufelnaser@subu.edu.tr

Mehmet Ali Hazar
mehmetalihazar@subu.edu.tr

Selçuk Coşkun
selcukcoskun@subu.edu.tr

Mustafa Çağrı Kutlu
mkutlu@subu.edu.tr

Gizem Hazar
gizemketenci@subu.edu.tr

1 Department of Mechatronics Engineering, Sakarya University of Applied Sciences, 54050 Sakarya, Turkey

2 Central Research Laboratory, Kastamonu University, 37100 Kastamonu, Turkey

3 Department of Electrical and Electronics Engineering, Sakarya University of Applied Sciences, 54050 Sakarya, Turkey

4 Department of System Engineering, Military Technological College, Muscat 111, Oman